SHOT NOISE LIMITED DETECTION OF OH USING THE TECHNIQUE OF LASER INDUCED FLUORESCENCE

Donovan M. Bakalyar, L. I. Davis, Jr., Chuan Guo, John V. James, Spiros Kakos, Peter T. Morris, and Charles C. Wang

This paper reports nearly shot-noise limited detection of OH using the technique of laser-induced fluorescence. A LIDAR-configuration is used to excite fluorescence in a large volume and a narrow-bandwidth interference filter provides spectral discrimination. This arrangement alleviates the effect of ozone interference and facilitates image processing at relatively close distances. The detection limit is determined mainly by the shot-noise of the solar background. Ground-based measurements in Dearborn indicate a detection limit of better than 1×10^6 OH/cm^3 over a forty-minute acquisition period. Under favorable conditions, a comparable detection limit was also observed for airborne measurements.

Donovan M. Bakalyar is with the Department of Physics, Oakland University, Rochester, Michigan 48063; Chuan Guo, Spiros Kakos, and Peter T. Morris are with Wayne State University, Detroit, Michigan 48202; the other authors are with Research Staff, Ford Motor Company, Dearborn, Michigan 48121-2053. Correspondence regarding this paper should be addressed to Charles C. Wang.

I. INTRODUCTION

Over the past ten years, the technique of laser-induced fluorescence [1] has been under intense development for possible measurements of the hydroxyl (OH) concentration in the troposphere. This activity reflects the belief that the hydroxyl radical plays a pivotal role in the chemical transformation of minority species in the troposphere, but its concentration there has not been established with any certainty. The range of daytime concentrations of OH is thought to be from 10^5 to 10^7 molecules/cm^3, depending on meteorological conditions and other parameters assumed in the model. This range is generally too low to be detected by conventional means. The technique of laser-induced fluorescence has promised unprecedented sensitivity and selectivity [3], but has proved to be susceptible to a number of interference problems [4], depending on the ambient conditions. The most serious interference encountered so far has been that arising from the photodissociation of ozone by the laser beam, leading to the production of metastable atomic oxygen [5]. Subsequent reaction with water molecule produces OH which is then detected by the same laser pulse. Under certain operating conditions, the level of this interference effect may be orders of magnitude higher than the OH concentration actually present in ambient air. This interference has been a serious problem in a number of field measurements [4, 6] undertaken without appropriate means to alleviate this effect. The technique [7, 8] which we have been developing takes advantage of the fact that the level of ozone interference is directly proportional to the intensity (watts/cm^2) used for excitation [4], and that it can be

reduced to a negligible level, without reducing the total fluorescence signal, by using a sufficiently large beam cross section for excitation.

The use of a large beam cross section naturally suggests a LIDAR-type configuration for collinear excitation and collection of fluorescence. Since OH is too reactive to allow conventional sampling, this LIDAR-type configuration allows the air to be measured in-situ. However, this configuration does allow comparatively high levels of solar radiation to be Rayleigh-scattered into the collection optics, and one must reduce the level of this solar background by appropriately terminating the line-of-sight of the telescope. For the system used in ground based measurements, the latter is accomplished with a baffled backstop, while for airborne measurements, the black-painted wingtip of the aircraft itself serves this purpose.

The use of spectral filtering is imperative in reducing the broadband solar background and the nonresonant fluorescence background, since the shot noise associated with this background determines the limit of OH detection. For the results reported in this paper, spectral filtering is done with a narrowband interference filter. Preliminary results obtained in Dearborn indicated a detection limit of better than 1×10^6 OH/cm^3 for ground-based operations of this system. A comparable detection limit was also observed for aircraft operations of this system under favorable conditions.

In Sections II and III, a brief description of the detection scheme and the experimental setup will be given. Section IV outlines the procedure

for data analysis. Results of OH measurements in Dearborn, as well as those from preliminary flights on board the NASA CV-990 aircraft, will be presented in Section V. New results on ozone interference will be presented and discussed in Section VI. Finally, in Section VII, the viability of our technique for OH measurements is discussed in light of these results.

II. DETECTION SCHEME

The technique of laser-induced fluorescence has been described in detail elsewhere [8]. It involves excitation of the OH radical using the $Q_1(2)$ line near 2,821 Å in the $^2\Pi(v'' = 0) \rightarrow {}^2\Sigma(v' = 1)$ transitions and observing the fluorescence emission associated with the $^2\Sigma(v' = 0) \rightarrow {}^2\Pi(v'' = 0)$ transitions near 3,090 Å. A successful application of this technique depends upon knowledge of the fluorescence spectrum and other physical and spectroscopic parameters involved in the absorption and reemission processes, many of which are now reasonably well documented in the literature [9 - 11]. The OH concentration and the fluorescence signal are related as follows:

$$(\text{OH signal}) = C \frac{\sigma_{0(OH)}}{\Delta\nu} \eta \, (\Delta n/n) \, [OH] \qquad (1)$$

Here (OH signal) is the fluorescence signal due to an OH concentration of [OH]; $\sigma_0(OH)$ and $\Delta\nu$ are the integrated absorption cross section and effective absorption linewidth of the exciting transition; and $\Delta n/n$ is the fraction of the OH population residing in the rotational level from which the exciting transition originates. In addition, C is a constant which is determined by the overall excitation and collection efficiencies. It can be evaluated most conveniently by noting that the spontaneous Raman scattering due to molecular nitrogen occurs around 3,020 Å, for which the excitation configuration and collection efficiencies are practically the same as those for OH fluorescence near 3,090 Å. Since this Raman signal is given by

$$(N_2 \text{ signal}) = C \, [N_2] \, \sigma_R(N_2) \qquad (2)$$

where $[N_2]$ is the ambient nitrogen concentration, and $\sigma_R(N_2)$ is the cross section for Raman scattering of nitrogen. Elimination of C in Eqs. (1) and (2) gives

$$[OH] = D \frac{(OH\ signal)}{(N_2\ signal)}\ OH/cm^3 \qquad (3)$$

where $D = \{\sigma_R(N_2)[N_2]\Delta\nu\ /\ \sigma_0(OH)\eta\ (\Delta n/n)\}$

as may be seen from Eqs. (1) and (2). Equation (3) describes a "normalization process" whereby the OH-fluorescence signal is normalized to that of the corresponding Raman scattering of nitrogen. In this manner, uncertainties in laser power, collection efficiencies, and some other parameters are eliminated from measurement results, thus improving the relative precision of the measurements. With the current best values for the parameters [8] substituted in Eq. (3), one calculates that

$$D = 2.4 \times 10^{10} P, \qquad (4)$$

where P is the ambient pressure in Bar. Based on the uncertainties of the parameter values used in evaluating D, we estimate the uncertainty in D to be on the order of 20% to 30%. It is evidently desirable to calibrate the fluorescence instrument used in OH measurements against some known source of OH under ambient conditions. One possible means for such a calibration is to make simultaneous measurements of OH in ambient air using both the fluorescence technique and the absorption technique. The possibility of using this scheme for calibration has been described elsewhere [12].

III. EXPERIMENTAL

Although the basic detection scheme remains unchanged, the present instrument package has incorporated a number of important improvements over that described previously [8]. Figure 1 depicts the present experimental setup used for both airborne and ground-based measurements of OH. The output from a doubled Nd-YAG laser is used to pump a tunable dye laser system consisting of an oscillator and an amplifier. The output from this dye laser system is sent through a crystal of deuterated KDP (Potassium Dihydrogen Phosphate) to generate second harmonic radiation near 2,821 Å. To assure that the exciting radiation is in resonance with the intended OH transition, a small portion of this second harmonic radiation is sent through a discharge cell containing water vapor, and the OH fluorescence excited therein is then detected by a photomultiplier. The main part of the second harmonic radiation is expanded and sent along the axis of a telescope, through a quartz aircraft window, to excite resonance fluorescence of OH in the outside air. The fluorescence light emitted in the backward direction is collected through the telescope, re-collimated, and directed toward a high-gain photomultiplier with appropriate filtering for detection near 3,090 Å. A portion of the re-collimated output from the telescope is split off, passed through an interference filter with a passing band near 3,020 Å, and detected by another photomultiplier in order to monitor the Raman signal of nitrogen.

For a given system of detection optics used to provide spectral discrimination, the telescope can be chosen to optimize the detection

sensitivity. Our system evolved around an 8" telescope with f/8 optics, which was originally chosen to interface with a 3/4-meter Spex spectrometer operated to provide a passing bandwidth of 30 Å. Optimal results were obtained with a sample volume extending from 50 feet to 130 feet away from the telescope. Under this arrangement, the demagnified image of the laser beam cross section is reduced sufficiently to be admitted by the spectrometer slit opening. However, this arrangement encounters some serious difficulties for aircraft operations when a large beam cross section is used. The sample volume extends only from 25 feet to 50 feet, and the demagnified image becomes too large for the spectrometer slit opening. To overcome this difficulty, the spectrometer has been replaced by a narrowband (24 Å), high transmission (~30%) interference filter with a dimaeter of 3".

For the measurements reported here, the laser was operated at ten pulses per second, and the laser output near 2,821 Å typically measured 2mJ in energy per pulse, about 7 nsec in duration, and 0.1 cm^{-1} in linewidth. With an effective beam cross section of 200 cm^2 or larger over the sampled region outside the aircraft, ozone interference was below the detection limit.

Under most operating conditions, solar background and, to a lesser extent, nonresonant fluorescence emitted by other absorbing species, proved to be undesirably large. To obtain an OH signal in the presence of this comparatively much larger background, the exciting radiation was tuned on and off the OH resonance after every ten laser shots, and the detection electronics were gated for about 70 nsec during the laser excitation. For diagnostic purposes, the solar background was also measured 2 microseconds

after each laser firing. These signals were processed with the aid of a CAMAC-based charge digitizer and stored in a HP-16 computer. Additionally, the laser power and the OH fluorescence signal excited in the water vapor discharge were processed and stored in a similar manner. In all, six signals were generated and stored for each laser pulse. After accumulation over 2,000 laser shots, the data were analyzed, the results of the analysis were printed on the CRT screen of the HP-16 and, at the discretion of the operator, the data would then be transferred to a disk for permanent storage. The process of accumulating data for 2,000 laser shots and performing related analysis took about four minutes.

It was desirable to verify independently that the entire detection system operated satisfactorily. In some of our ground-based experiments, this was done by placing a small propane torch near the path of the exciting laser beam. By adjusting the position of the flame, an OH signal equivalent to an average concentration ranging from high 10^6 to 10^9 OH/cm^3 over the region of excitation, could be easily observed. As will be described in a later section, an unexpanded laser beam also generates enough ozone interference in the range of 10^7 to 10^8 OH/cm^3 to verify that our system is working.

IV. DATA PROCESSING AND ANALYSIS

The analysis procedure to be outlined below is aimed at extracting the OH fluorescence signal from the vastly larger solar background and the nonresonant fluorescent background emitted by other absorbing species. For simplicity, we have opted to analyze our data using statistical techniques appropriate for stationary processes. Recognizing that the background levels and other quantities measured vary with time, we have chosen sufficiently short time intervals for acquisition and analysis of data so that the assumption of stationary processes is reasonable.

It is convenient to cast the various signals observed in our experiments in a form frequently employed in statistics. When the laser frequency is tuned in resonance with the desired OH transition, the observed signal near 3090 Å, y_1, is given by

$$y_1 = [\text{Solar}] + [\text{NRF}]x_1 + [\text{OH}]x_1 \qquad (5)$$

where x_1 is the corresponding laser power, [Solar] represents the solar background within the detection bandwidth, $[\text{NRF}]x_1$ is the nonresonant fluorescence background, and $[\text{OH}]x_1$ is the fluorescence signal due to OH. Similarly, when the laser frequency is off resonance, the corresponding signal, y_2, is given by

$$y_2 = [\text{Solar}] + [\text{NRF}]x_2 \qquad (6)$$

where x_2 is the laser power for off-resonant excitation. Subtraction of Eq. (6) from Eq. (5) gives

$$y_3 = [OH]x_1 + [NRF]x_3 \tag{7}$$

$$y_3 = y_1 - y_2 \tag{8}$$

$$x_3 = x_1 - x_2 \tag{9}$$

Equation (7) describes a linear equation whose two parameters can be determined through a least-squares fit according to standard procedures [15]. Accordingly, the OH concentration is given by

$$[OH] = \{[y_3x_1][x_3^2] - [x_1x_3][y_3x_3]\} / \Delta \tag{10}$$

$$\Delta = [x_1^2][x_3^2] - [x_1x_3]^2 \tag{11}$$

and the corresponding variance is given by

$$V(OH) = s^2 [s_3^2] / \Delta \ . \tag{12}$$

Here the square brackets denote the sum of the products of the quantities therein over the set of observations and s^2 is the sample variance. Since the laser operates for ten shots between frequency switching and there are a total of 2,000 laser shots per run, one may form from each run 100 groups, each of which contains ten pairs of on-off observations, and apply the above equations to each group. The resulting 100 OH values are then processed in the usual manner to yield a mean value and standard deviation.

V. PRELIMINARY RESULTS

To ascertain the validity of the statistical analysis of the previous section, a number of tests may be performed on the data. First of all, the possibility that the data are shot-noise limited may be tested by plotting uncertainty versus data level. In Fig. 2, the noise level computed according to Eq. (12) is plotted as a function of the total signal level (solar plus fluorescence) observed near 3,090 Å in the experiments. As stated previously, each data point represents the average for a run of 2,000 laser shots. A least-squares fitting of these results yields a slope of 0.59 ± 0.02, as may be compared to a slope of 0.5 for purely shot-noise limited detection. This dependence indicates that the noise associated with these signals is largely shot-noise-like, but with perhaps a small component linearly proportional to the background level. This latter component is due most likely to the changing background level, which contributed to Eq. (12) through incomplete cancellation between on- and off-resonance readings. Despite this lack of complete cancellation, it should be possible to realize further improvements in the signal-to-noise by averaging over longer periods of data acquisition.

To determine whether V(OH), as derived from Eq. (12), is an appropriate statistic for these measurements, it is useful to look at the distribution of OH values given by Eq. (10) when the sample average for these values is nearly zero. This distribution should center around zero with a width proportional to the standard deviation of Eq. (12). Figure 3a depicts the histogram for such a distribution. Here the level of OH signal

is expressed in units of the standard deviation of the distribution and the number of occurrences of a given level is plotted as a function of this level. The data points in Fig. 3a each represent a value deduced from Eq. (10). The distribution of these points is seen to be approximately symmetric and has a mean value well within the standard deviation of the mean. It is also seen that, of the total of 400 data points, 293 (or 73%) are located within one standard deviation from the center of the distribution. This may be compared to the case of a normal distribution, for which roughly 68% fall within one standard deviation. The number of points lying between one and two standard deviations, and beyond two standard deviations away from the center, represent about 20% and 6%, respectively; these values are not quite the same, but are comparable to the corresponding values of 29% and 2% for a normal distribution. We are unsure of the cause for this deviation from normal distribution, but it is very likely that this apparent deviation is due to inclusion of data points far out in the wings of the distribution in Fig. 3a, which are often associated with high background levels. If these points are excluded in the computation, the standard deviation for the distribution in Fig. 3a would become less by a factor of 1.3, and the shape would also approximate more closely that of a normal distribution.

As a further attempt to elucidate the nature of the distribution and to demonstrate that our system is free from any bias arising from possible inbalance in the wavelength tuning, extensive measurements were made at night or at high altitudes under very dry conditions when little OH was expected.

The results of these measurements are shown in Fig. 3b, where the level of OH signal averaged over a run of 2,000 laser shots is expressed in units of the associated standard deviation for the run, and the number of occurrences of a given signal level is plotted as a function of that level. This distribution in Fig. 3b is also seen to be approximately normal and centered around zero, and the width of the distribution is approximately one (standard deviation). Based on these observations, it is concluded that the statistical analysis as outlined in the last section is applicable to the results of our experiments, and the standard deviation as computed in Eq. (12) is a reasonable, albeit conservative, estimate of the uncertainties in the experimental determination.

Table I summarizes the results of ground-based OH measurements conducted on September 17, 1983 in Dearborn, Michigan. For each of the time periods listed, the value of OH concentration represents the average of ten runs each containing 2,000 laser shots. It is seen that, for the period near local noon, the signal is statistically significant. However, no OH signal discernible from the statistical uncertainty was observed for other periods. (It should be pointed out that, while it was sunny at noon, clouds which moved in during the afternoon undoubtedly accounted for some of the lack of signal during that time.) The OH signal averaged over the entire monitoring period may be calculated from the table to be $(0.61 \pm 0.29) \times 10^6$ OH/cm^3.

The last row in Table I was obtained with an unexpanded beam, and the corresponding signal should be due entirely to ozone interference.

However, for normal monitoring during the periods listed, the laser beam was expanded by about a factor of 400 in area. One would thus expect that the ozone interference level should be on the order of $110 \times 10^6 / 400 = 0.27 \times 10^6$ OH/cm^3 when comparable ozone and water levels were involved during monitoring. This level is lower than the detection limits listed in Table I by about a factor of two.

VI. OZONE INTERFERENCE

Ozone interference involves dissociation of ozone molecules following absorption of the uv radiation used for exciting the resonance fluorescence of OH. The dissociation products of ozone are molecular oxygen and metastable atomic oxygen $O(^1D)$. Under ambient conditions, most of the metastable oxygen atoms thus formed are de-excited to the ground state through collisions with nitrogen and oxygen molecules, but a small fraction reacts with water molecules to form OH in the ground electronic state. It is shown on the basis of a rate equation analysis [5] that the average OH concentration generated and "seen" by a square-top laser pulse is given by

$$[OH] = [OH]_s \{F(B\Delta t) - (B/A)F(A\Delta t)\}/(1 - B/A) \quad (13)$$

$$\text{with } [OH]_s = (1/A)\,\sigma_o\, k[H_2O][O_3]E \quad (14)$$

$$\text{and } F(x) = 1 - (2/x)[1-(1/x)(1 - e^{-x})] \quad (15)$$

Here the bracketed quantities refer to concentrations of the various species involved; A and B are, respectively, the rate of de-excitation of $O(^1D)$ and the rate of rotational relaxation of the generated OH, both constants being proportional to the partial pressure of the various species present in the excitation region; σ_o is the absorption cross section; E is the energy per unit area per pulse; and Δt is the laser pulsewidth.

In order to apply Eq. (13) to actual experiments, it was conjectured [7] that the population in a given low-lying rotational level consists of a component resulting from exchange of energy with the translational

degree of freedom [13], and another component due to rotational relaxation from higher rotational levels into which OH molecules are first formed as the reaction product of $O(^1D)$ and water. The former component is associated with a relaxation rate comparable to A, but the latter component may be associated with much longer rotational relaxation times since cascade processes from one rotational level to another are involved. To the extent that this latter component is small, Eq. (13) may be simplified to become

$$(OH] = \{A'_c F(A t)\} [OH] \qquad (16)$$

where A'_c is the fraction of the OH population generated in the particular rotational level from which absorption originates. The product $A'_c F(A\Delta t)$ embodies the correction from steady-state results, and may be identified with the correction factor introduced previously [8].

In Fig. 4, Eq. (15) is shown graphically. It has been noted previously [7] that $F(A\Delta t) \sim 0.8$ for a 10 nanosecond laser at ambient pressure. Moreover, this function may decrease drastically as the pressure and/or pulsewidth is reduced. For example, when the pressure is reduced to 1% of the ambient for a 10 nanosecond laser, a comparable decrease in the value of F(x) is noted. This decrease with pressure forms the basis for interference reduction in some of the detection schemes which have been proposed [14].

Taking advantage of the fact that water vapor and ozone concentrations were measured concurrently with our airborne measurements of OH, we have made a re-determination of this correction factor. Excluding those runs for which reliable water vapor measurements were not available, the

results of our ozone interference measurements are shown in Fig. 5 as a function of the product of ozone and water vapor concentrations divided by the ambient pressure. These measurements are seen to follow a linear dependence as expected; the scattering of data is due in part to the uncertainty in the measurements of the water vapor, the statistical uncertainties of the OH signal computed, and to a lesser extent, fluctuations in the value of other parameters such as the laser power. The correction factor for Eq. (16) is determined from these data to be 0.1 ± 0.01 with possibly an additional uncertainty of 20% due to factors discussed in Section II. This new value is consistent with the value 0.1 ± 0.05 determined previously.

VII. CONCLUSIONS AND DISCUSSION

Using a tunable laser system combined with a terminated telescope path and a narrowband interference filter, we have demonstrated a working scheme for measurements of OH in ambient air. With the laser system operating at 10 Hz, the integration time needed in order to obtain a detection limit of about 10^6 is typically about 40 minutes. A correspondingly shorter integration time would be possible if a higher pulse repetition rate is implemented for the laser system.

For measurements in moderately clean air at ground level, the background signal consists mainly of solar radiation Rayleigh-scattered into the collection optics. For airborne operations, the black-painted wing tip used to terminate the line-of-sight of the telescope also scatters a significant amount of additional light into the collection optics, increasing the background signal by as much as a factor of ten under adverse conditions.

As may be seen from the results presented in the previous sections, our system appears to be free from systematic bias. Analysis of the null results also indicates that our detection limit is determined essentially by the shot-noise associated with the background signal. For ground-based operations, a detection limit of better than 1×10^6 OH/cm^3 was demonstrated in Dearborn. For airborne operations, the detection limit may be comparable under favorable conditions, but may be degraded by as much as a factor of four if an adverse solar angle relative to the detection optics is encountered.

As part of the flight measurements, we have redetermined the numerical factor used in computing the level of ozone interference. The results

are in agreement with the less accurate results determined previously, and are also consistent with the published theoretical account of the phenomenon.

The detection sensitivity which we have demonstrated in our experiments should be sufficient for routine measurements in areas where the OH concentration is in the range of high 10^6 molecules/cm^3 or higher. Indeed, we have performed OH measurements in the Intertropical Convergence Zone (ITCZ) near the South Pacific, and in such moderately polluted areas as the San Joaquin Valley. The results of these measurements will be published elsewhere.

It should be noted that the detection sensitivity for the system configuration described in this paper could, in principle, be improved by using narrower detection bandwidth. The idea is to discriminate more against the continuous spectrum of solar background in favor of the groups of discrete OH fluorescence lines. For shot-noise limited detection, however, any apparent advantage may be offset by the difference in the way the signal-to-noise ratio depends on the levels of OH signal and solar background. The signal-to-noise ratio is proportional to the level of OH signal, but is proportional to the inverse square root of the background level. Consider, for example, reducing the bandwidth by a factor of 100. To the extent that the solar spectrum is flat over the spectral range of interest, this reduction would lower the solar background by the same amount, but would lower the associated shot noise by a factor of ten only. Consequently, any concomitant reduction in the OH signal must be kept less than a factor of ten in order to realize any improvement in the signal-to-noise ratio. In practice, the use of a narrower bandwidth for detection also necessitates a reduction of the usable

solid angle for collection, resulting in a reduction of the throughput (etendue) of the collection optics. Based on the fluorescence spectrum of OH, we estimate that a detection bandwidth of 20 cm^{-1} would be optimal and would give a signal-to-noise ratio slightly better than that described in this paper. A much narrower bandwidth would be impractical in terms of the solid angle for collection, and would reduce the signal-to-noise ratio even if it could be implemented.

It would be desirable to achieve another order of magnitude improvement either in enhanced sensitivity or in reduced integration time so as to facilitate routine measurements in clean air at the ground level where the OH concentration may be very low. An improvement of this magnitude would be possible if measurements could be performed at pressures lower than about 7 torr. This possibility can be understood through an examination of Eq. (16) and Fig. 5, which indicate that the ozone interference level at this reduced pressure will be reduced by about two orders of magnitude while the fluorescence efficiency is increased by the same amount. Lowering the system pressure clearly requires sampling the air by some means without contaminating the air or affecting the relative concentration of OH. It is not clear such a means can be found easily.

It is a pleasure to acknowledge the cooperation of Barr Associates, Inc. of Westford, Massachusetts, in supplying the narrowband interference filters described in this paper. Their timely delivery of these outstanding filters contributed to the success of the experiment. This research has been supported in part by National Aeronautics and Space Administration through Wayne State University and by the Department of Energy. The flight measurements were taken as a part of the GTE-CITE mission sponsored and administered by NASA, and the ozone data used in Fig. 5 were kindly provided by Dr. G. Gregory.

REFERENCES

1. C. C. Wang, Bull. Am. Phys. Soc. 19, 24 (1974); C. C. Wang and L. I. Davis, Jr., Phys. Rev. Lett. 32, 349 (1974).

2. See, for example, P. J. Crutzen and L. T. Gidel, J. Geophys. Res. 88, 6641 (1983), and references cited therein.

3. D. K. Killinger, C. C. Wang, and M. Hanabusa, Phys. Rev. A13, 2145 (1976).

4. C. C. Wang, L. I. Davis, Jr., C. H. Wu, and S. Japar, Appl. Phys. Lett. 28, 14 (1976).

5. M. Hanabusa, C. C. Wang, S. Japar, D. K. Killinger, and W. Fisher, J. Chem. Phys. 66, 2118 (1977).

6. (Williamsburg Conference - Bradshaw, Rodgers, & D^3).

7. C. C. Wang and L. I. Davis, Jr., Geophys. Res. Lett. 9, 98 (1982); L. I. Davis, Jr., C. C. Wang, X. Tang, H. Niki and B. Weinstock, 2nd Symposium on the Composition of the Non-Urban Troposphere, Williamsburg, Virginia, (1982).

8. C. C. Wang, L. I. Davis, Jr., P. M. Selzer, and R. Munoz, J. Geophys. Res. 86C, 1181 (1981).

9. C. C. Wang, M. T. Meyers, and D. Zhou, Phys. Rev. Lett. 47, 490 (1981).

10. K. R. German, J. Chem. Phys. 64, 4065 (1976).

11. R. K. Lengel and D. R. Crosley, J. Chem. Phys. 67, 2085 (1977); 68, 5309 (1978).

12. D. M. Bakalyar, J. V. James, and C. C. Wang, Appl. Opt. 21, 2901 (1982).

13. K. H. Gericke and F. J. Comes, Chem. Phys. Lett. 74, 63 (1980).

14. T. M. Hard, R. J. O'Brien, T. B. Cook, and G. A. Tsongas, Appl. Opt. 18, 3216 (1979).

15. G. E. P. Box, W. G. Hunter, and J. S. Hunter, "Statistics for Experimenters", John Wiley & Sons, New York, 1978.

Table I. Summary of results of OH measurements on September 17, 1983 in Dearborn, Michigan. The last row marked with an asterisk in the table represents values obtained with an unexpanded laser beam; they should be due entirely to ozone interference.

Time (EDT)	OH (10^6 molecules/cm^3)
11:49 - 12:31	0.27 ± 0.68
13:03 - 13:54	2.0 ± 0.68
14:32 - 15:16	0.58 ± 0.63
15:58 - 16:43	0.56 ± 0.63
17:37 - 18:23	-0.34 ± 0.63
18:46 - 18:54*	110 ± 2

FIGURE CAPTIONS

Figure 1. Schematic of the experiment.

Figure 2. Logarithmic plot of the noise on the OH signal as a function of the overall signal level. The noise is the fluctuation of the signal about its mean value as calculated according to Eq. (12). See text for more details.

Figure 3. (a) Histogram for the distribution of a sample of OH measurements for which the sample average was nearly zero. Each data point represents an OH value deduced according to Eq. (10) from 20 laser shots over a period of two seconds.

(b) Histogram for the distribution of null results obtained during night flights and flights during which no OH was expected. As may be contrasted with the results in Fig. 3a, each data point here represents an average OH value associated with 2,000 laser shots or 200 seconds.

Figure 4. Plot of F(x) in Eq. (15) as a function of the dimensionless variable x.

Figure 5. Plot of ozone interference signal as a function of the product of ozone (in ppbv) and water vapor (in mb) divided by the ambient pressure (in 1000mb).

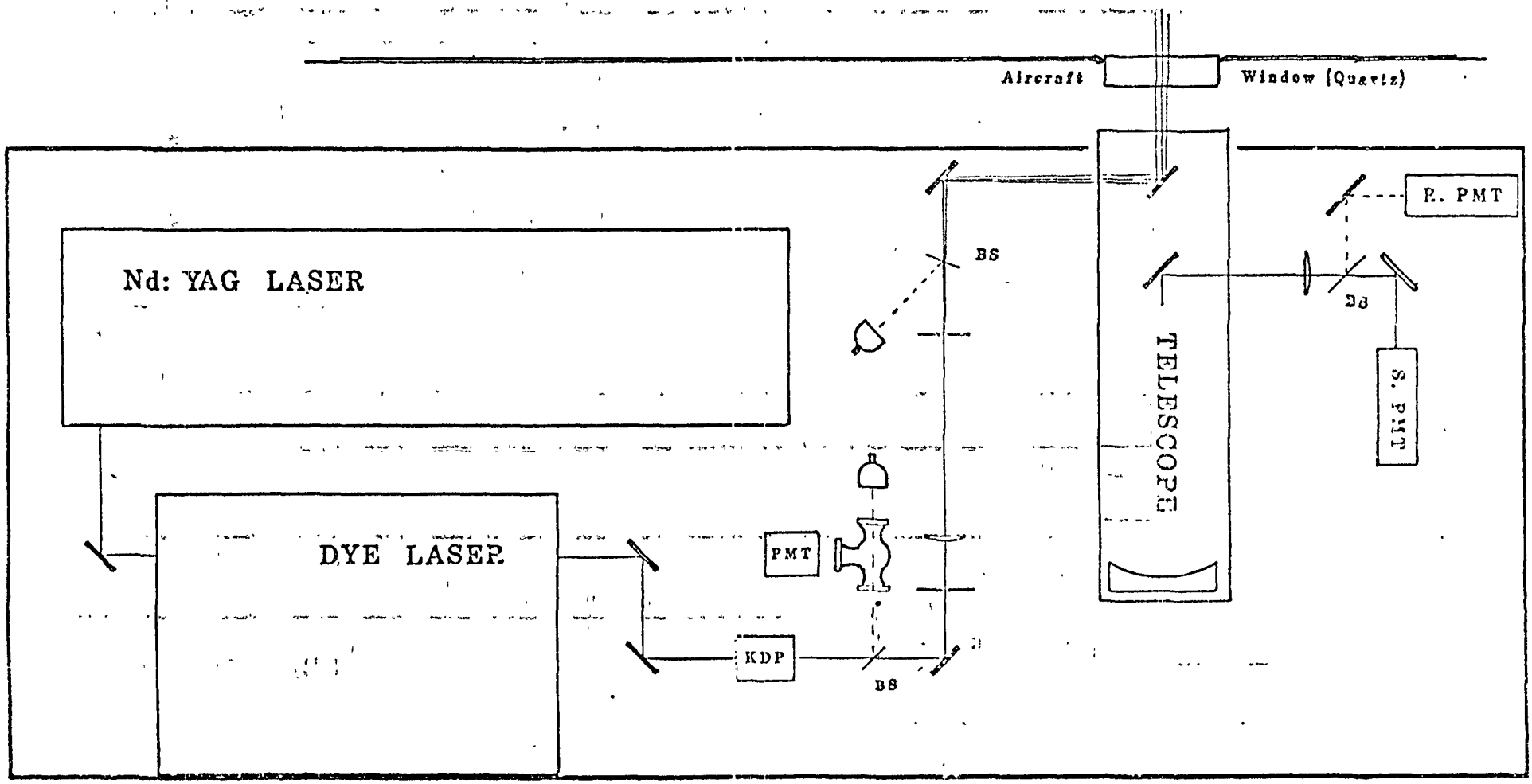
Aircraft
Window (Quartz)
Nd: YAG LASER
DYE LASER
BS
PMT
KDP
BS
TELESCOPE
R. PMT
BS
S. PMT

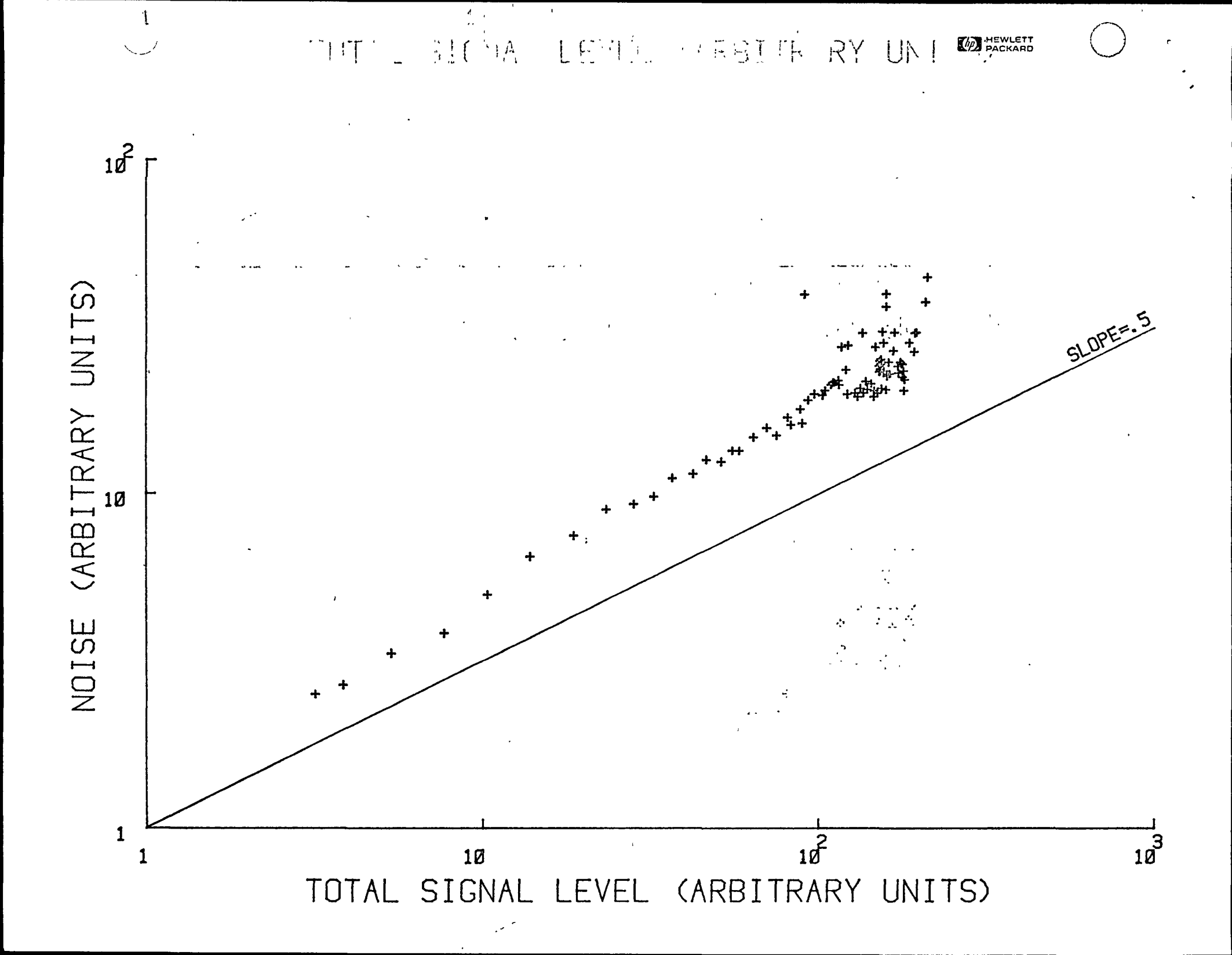
HEWLETT PACKARD
NOISE (ARBITRARY UNITS)
TOTAL SIGNAL LEVEL (ARBITRARY UNITS)
SLOPE=.5
1
10
10^2
1
10
10^2
10^3

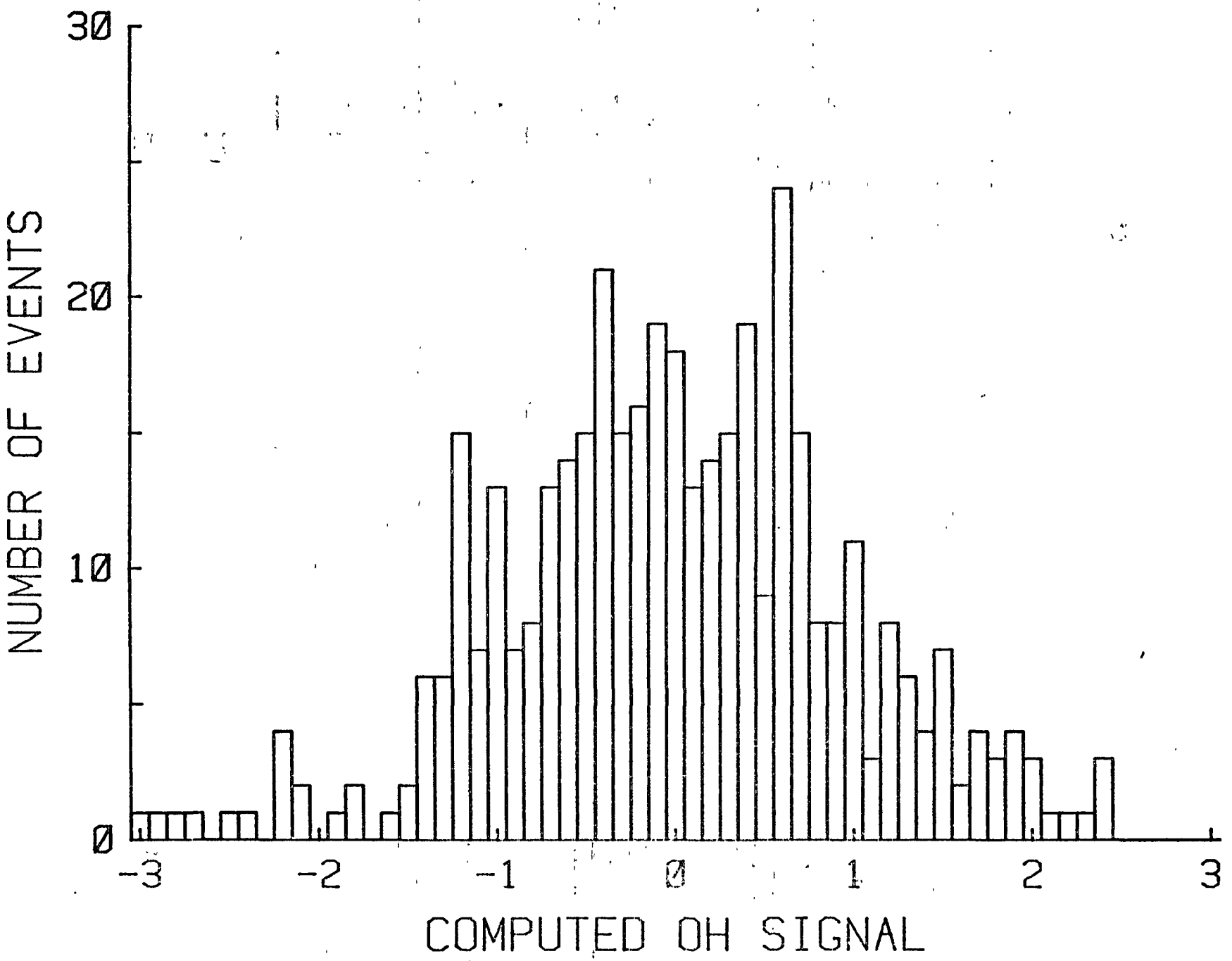
30
20
10
0
NUMBER OF EVENTS
-3
-2
-1
0
1
2
3
COMPUTED OH SIGNAL

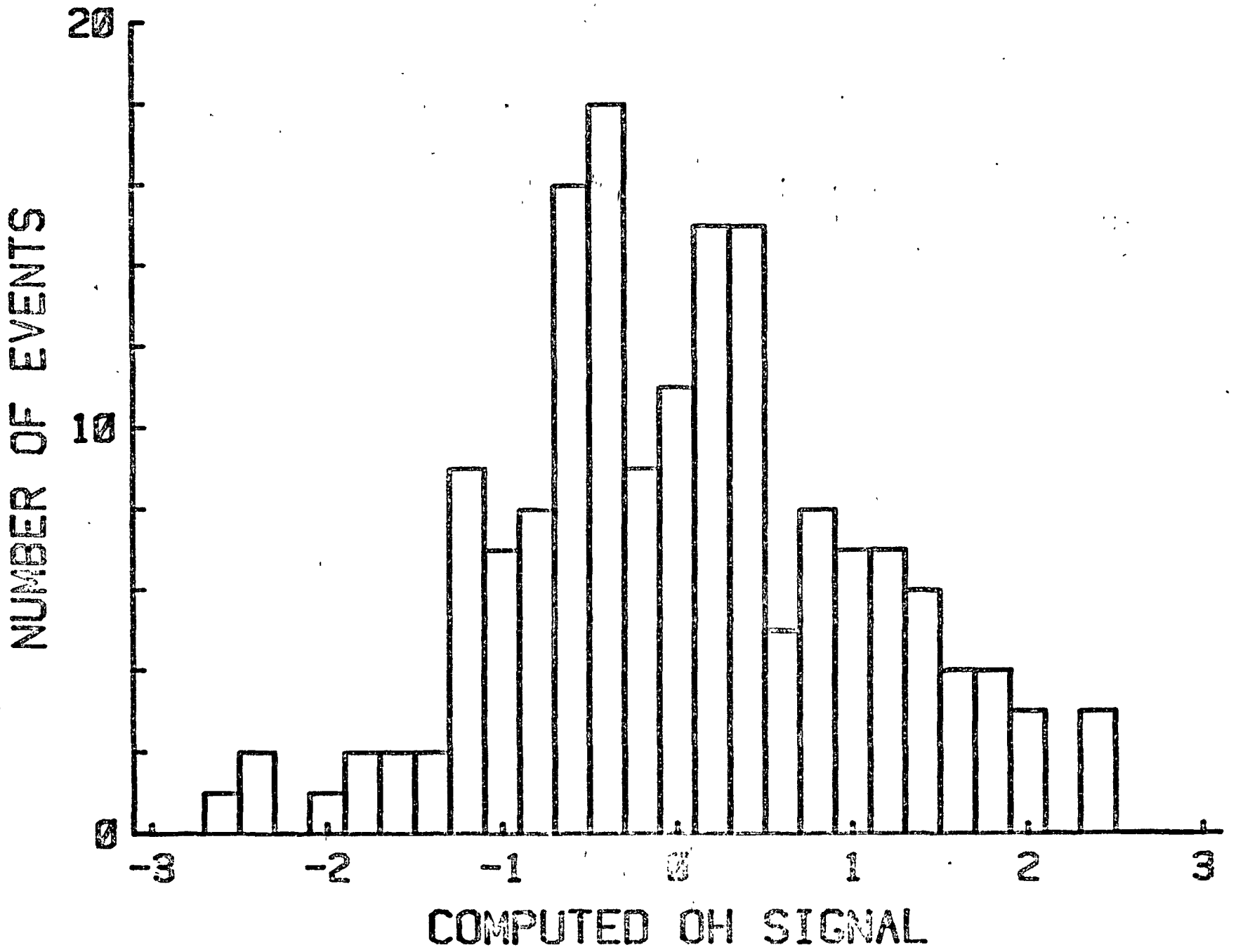
HEWLETT PACKARD
NUMBER OF EVENTS
20
10
0
-3
-2
-1
0
1
2
3
COMPUTED OH SIGNAL

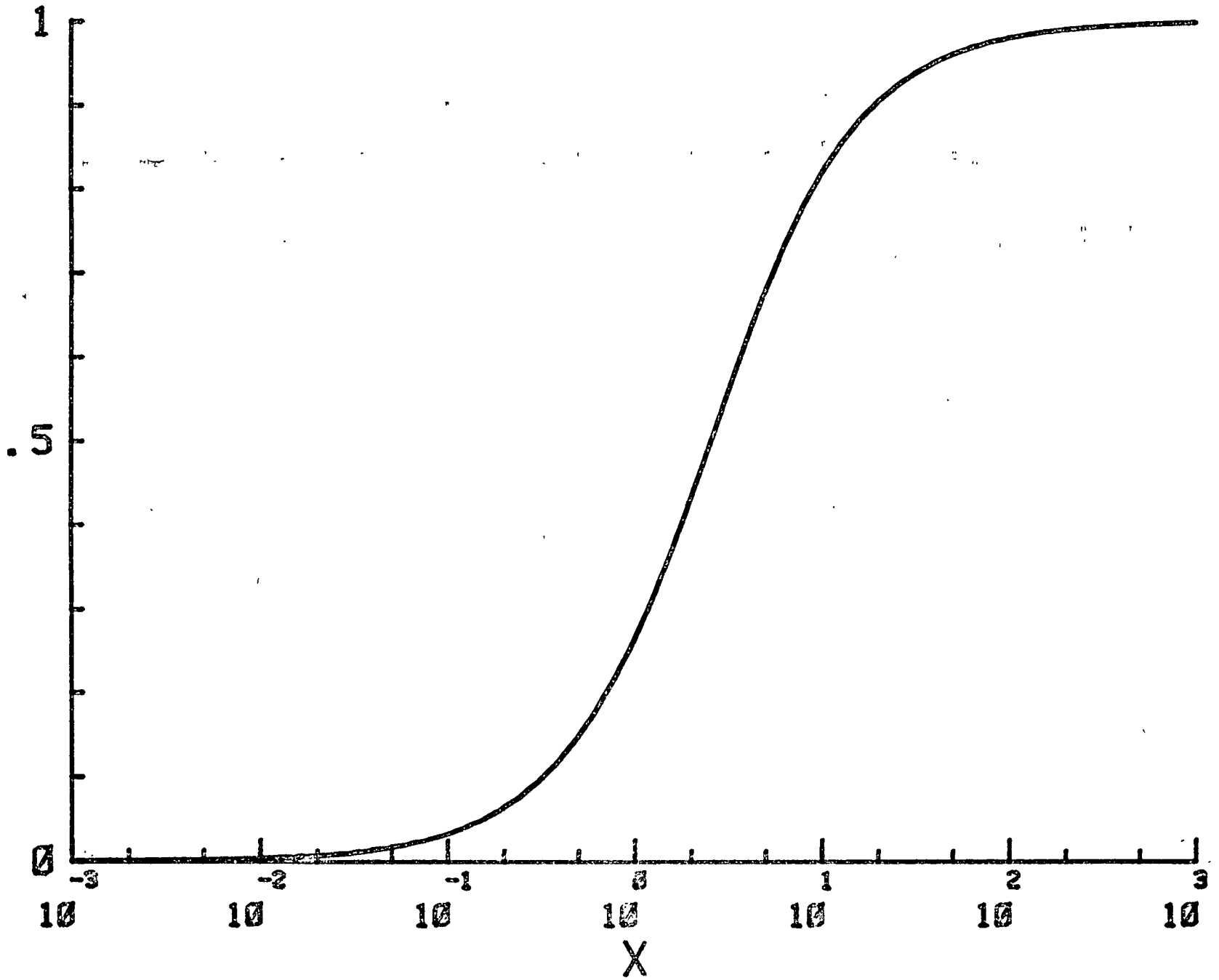
1
.5
0
10^-3
10^-2
10^-1
10^0
10^1
10^2
10^3
X

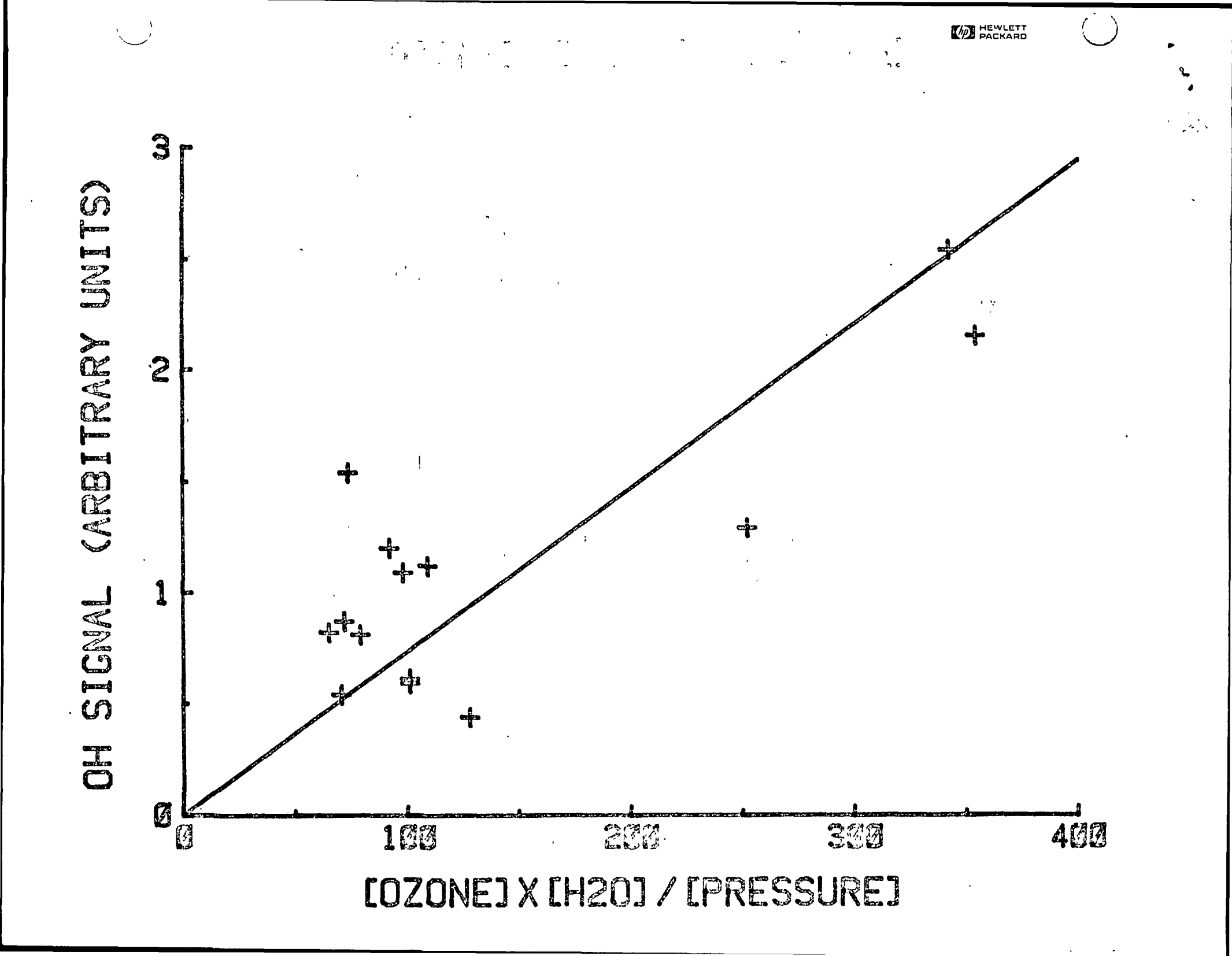
HEWLETT PACKARD
OH SIGNAL (ARBITRARY UNITS)
3
2
1
0
0
100
200
300
400
[OZONE] X [H20] / [PRESSURE]